

DRAINAGE CURVE MEASUREMENTS IN DUAL SCALE FIBER REINFORCEMENTS

Markus Nordlund¹, Véronique Michaud^{1,2}, and Jan-Anders E. Månson¹

*Ecole Polytechnique Fédérale de Lausanne (EPFL), Laboratoire de Technologie des Composites
et Polymères (LTC), Station 12, CH 1015 Lausanne, Switzerland
Corresponding author's Email: veronique.michaud@epfl.ch*

SUMMARY: A methodology is presented to determine the saturation curve of a resin/glass fabric system, during infiltration in a transparent mould under constant flow rate. Video acquisitions are transformed by image analysis into saturation level versus position and time, and coupled to inlet pressure measurements. A numerical multiphase flow model is then used to simulate the infiltration for various combinations of drainage curve parameters. The numerical parameters to describe the saturation and relative permeability are determined by response surface optimization. The drainage curve and relative permeability expression determined at one time are shown to adequately describe the entire injection process.

KEYWORDS: wettability, numerical analysis, Liquid Composite Molding (LCM), unsaturated flow

INTRODUCTION

In liquid composite molding (LCM), capillary phenomena take place at the flow front where the resin progressively replaces the air during the injection. This phenomenon is often neglected in modeling of the LCM process, since the surface tension of the resin is generally low. In structured fiber reinforcements, where the fibers are collected in bundles with an interbundle spacing between them, two geometrical scales influence the resin flow. Inside the fiber bundles, the permeability is low and the effect of the surface tension is high due to the small pore radius, whereas it is the opposite in the inter-bundle spacing. These differences result in an uneven flow front as observed in many cases [1-5]. When modeling the flow front progression, it is thus necessary to take this into account, in particular as it may lead to voids in the final part. To avoid treating the issue at the scale of the bundles, the unevenness of the flow front can be considered as an unsaturated region in a continuum mechanics model, as developed in soil science [6-8]. This approach has so far not been investigated fully for liquid composite moulding processes. A main issue is the need to know the saturation versus pressure relationship, known as the drainage-

imbibition curve in soil science, and the related relative permeability dependence on saturation. This relationship is not straightforward to model because it requires a good knowledge of the porous medium geometric characteristics [9]. In general, in soil science, it is experimentally determined by measuring the saturation in the porous medium for each level of applied static pressure [6, 7, 10-12]. This method was applied to drainage curve measurement in metal matrix composite processing with good success [13-16]. For polymer composites, saturation curves were measured with oil [17]. The resulting saturation curves are thereafter fitted to semi-empirical equations [18, 19], which are then used in the multiphase flow modelling of the infiltration [15, 16, 20]. In bimodal porous media, and for viscous resins, such as those used in LCM, the dynamic wetting behaviour is, however, strongly dependent on the injection velocity, and on the nature of the resin. It was shown in [17, 21] that the flow can either lead in the tows or in the inter tow region depending on the injection velocity. Static methods as described previously may not describe these effects, since they assume that the saturation versus capillary pressure relationship is independent of the injection velocity. Attempts were performed to dynamically measure the saturation during injection, either using electrical conductivity or image analysis [22, 23]. These were however not linked to drainage curves. In this work, we propose a methodology to measure the drainage curve of a resin/fabric system, during infiltration in a transparent mould under constant flow rate by coupling image analysis of video acquisitions during flow with a numerical optimization routine to determine the parameters of the drainage curve and the relative permeability.

THEORY

By similarity with soil mechanics, we define the effective saturation S of fluid phase α as:

$$S_\alpha = \frac{\theta_\alpha}{(1 - V_f)}, \quad (1)$$

where θ_α is the volume fraction of fluid phase α in the porous medium and V_f the fibre volume fraction of the reinforcement. It is generally assumed that the densities of liquid and solid phases are constant, which in most cases of non-reactive infiltration is a reasonable assumption. Assuming that the air phase remains at a pressure close to atmospheric pressure, the system of equations describing the unsaturated injection of resin into fibre preforms is reduced to Richard's equation, given below (see [24] for details):

$$C \frac{\partial p_\alpha}{\partial t} + \nabla \cdot \left[-\frac{\overline{\overline{K}}_s k_{r,\alpha}}{\eta_\alpha} \cdot (\nabla p_\alpha + \rho_\alpha g \nabla z) \right] = 0, \quad (2)$$

where α now stands for the resin phase and $C = \theta_s \cdot \partial S_\alpha / \partial p_\alpha$ is the resin capacity. Initial and boundary conditions valid for each case complete the definition of this non-linear problem.

The main characteristics of the fibre preform and of the fluid are: (i) the viscosity η_α assumed to be constant over the duration of the flow front progression; (ii) $S_\alpha(p_\alpha)$, a function governed by capillarity; (iii) $\overline{\overline{K}}_s$, the permeability tensor, which depends on the local value of V_f , and the fabric architecture and $k_{r,\alpha}$, the relative permeability, which depends on the saturation S_α . The functions (ii) and (iii) are not known a priori, and are often determined experimentally as indicated in Soil Science literature [6, 7, 10-12]. For instance, Brooks and Corey developed a

semi-empirical relationship [31], which has been shown to describe well the saturation of soils [9]. Similarly, a semi-empirical expression, more suited for numerical simulations has also been developed by van Genuchten and Mualem [19, 25] and is given as:

$$S_{mw} = \begin{cases} 1 - \frac{1}{\left[1 + \beta \left| \frac{p_{nw}}{\rho_{nw} g} \right|^N\right]^M}, & p_{nw} > 0 \\ 0, & p_{nw} \leq 0 \end{cases}, \quad (3)$$

$$k_{r,nw} = \begin{cases} S_{mw}^L \left(1 - (1 - S_{mw})^{\frac{1}{M}}\right)^{2M}, & p_{nw} > 0 \\ 0, & p_{nw} \leq 0 \end{cases}, \quad (4)$$

for a non-wetting fluid, where L , N and β are the van Genuchten parameters and $M = 1 - 1/N$. From here on, the fluid is assumed to be non-wetting and the sub-index nw will be excluded to simplify the writing. Similar analysis can be done for wetting fluids.

The system to solve is highly nonlinear, since both S_α and $k_{r,\alpha}$ are function of pressure. In this work, the Finite Difference (FD) method was used to solve for pressure as a function of z and t . A 1D model was developed to simulate the unidirectional flow occurring during the preform injection [24]. To complete the problem description, a flux boundary condition was defined at the inlet to represent the constant flow rate, whereas a zero flux condition was applied at the outlet boundary. The initial condition required to complete the problem is the pressure, since both C and K depend on S , which in turn depends on p . For the numerical stability, the initial pressure field, p_{init} was chosen so that the initial saturation field, S_{init} , was nonzero but small ($S_{init}=0.001$ in the present work).

METHODOLOGY

In order to determine the relationship between the saturation and the capillary pressure, $S(p)$, an injection is conducted under constant flow rate in a transparent mould. The flow propagation through the fabric is video filmed by a digital camera and the pressure is measured at the inlet of the mould with a pressure transducer. Hence, the output data from the injection is a video sequence of the flow propagation and the measurement of inlet pressure as a function of time.

The frames from the video acquisition are treated by image analysis, in order to determine $S(z, t_i)$. As observed in many fabric infiltration experiments [1-5], three zones are in general observed: a fully saturated zone near the resin inlet, a partially saturated zone, and the dry fabric. The pressure in the resin phase at every position z is needed, in order to establish the relationship, $S(p)$. The only two positions where the correspondence between z and p can be made from the acquired experimental data are: (i) directly in front of the unsaturated region, z_0 , where the pressure is atmospheric, and at the end of the unsaturated region, z_f , where the saturation is $S_f = 0.99$, cf. Fig. 1. There, the pressure p_f can be calculated using Darcy's law for saturated flow as:

$$p_f = p_{in} - \frac{Q L_{sat}}{A} \frac{\eta}{K_s} - \rho g z, \quad (5)$$

where L_{sat} is the length of the fabric, which has full saturation measured from the video frame at time t_i , and z is the vertical distance from the beginning of the fabric to the beginning of the

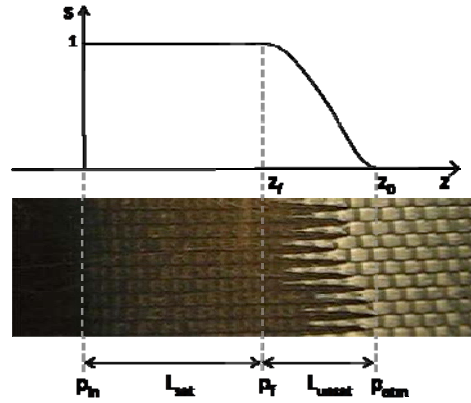


Fig. 1 Typical $S(z, t_i)$ curve related to the saturated and unsaturated regions observed in the video frame of the experiment.

unsaturated region. The flow rate Q is calculated by image analysis of the video frames, the cross-sectional area A is calculated from the fabric dimensions measured prior to the injection and the ratio between the viscosity and the saturated permeability in the flow direction and η/K_s is calculated from slope of the measured inlet pressure curve, assuming that the influence of the unsaturated zone resistance is negligible for well developed infiltration zones [5]. Furthermore, $p_{\text{in}}(t_i)$ is taken from the inlet pressure curve with the assumption that the pressure at the beginning of the fabric is uniform, the flow is unidirectional and that it behaves linearly according to Darcy's law over the saturated region.

Equation (3) and (4) are used to determine how the pressure varies over the unsaturated region. Three parameters N , L , β , need to be determined. This was achieved by numerical simulation of the unsaturated flow, performed for the same injection condition as in the experiment. The resulting $S(z, t_i)$ data from the numerical simulation were thereafter compared to the experimental $S(z, t_i)$ data to investigate the appropriateness of the choice of N , L , β . An optimization procedure [24] was conducted to determine the optimal fit between the numerical and experimental $S(z, t_i)$ data. Finally, knowing the optimal value of the parameters, N_{opt} , L_{opt} and β_{opt} , the proper $S(p)$ and $k_r(S)$ relationships were determined.

EXPERIMENTS

The resin used was a commercial, two component system Epikote 828LV epoxy resin and Epikure DX 6514 hardener from Shell. Data for the epoxy system are given in [26]. The mixing ratio for this system was 100:17 parts by weight of base and hardener, respectively. The density of the mixture was measured to be 1020.4 kgm^{-3} . The curing kinetics of the epoxy system was studied at 80°C , and it was found that viscosity remained constant during the injection time of the mixed resin at around $0.075 \text{ Pa}\cdot\text{s}$. The fibre reinforcement studied in the present work was a glass fibre fabric, with epoxy compatible sizing, with an area weight of 0.424 kgm^{-2} and a UD dominated architecture.

In the RTM experiments, one layer of the unidirectional glass fibre fabric was placed into a flat mould consisting of a lower part made of steel and an upper part made of glass reinforced by a steel frame. This transparent mould was heated with six evenly distributed computer controlled heat cartridges. The temperature of the mould was set to a temperature of 80°C. The gap between the lower and the upper part of the mould was controlled by inserting metal frames of desired thickness. The dimensions of the injected parts were 0.10 m x 0.10 m x 0.2 mm, leading to a volume fraction, $V_f \approx 57.2\%$. In order to avoid race tracking at the sides of the fabric, the fabric lay-up was sealed with sealing tape. Furthermore, the mould was raised to a vertical position in order to facilitate video acquisition of the flow front propagation through the transparent upper mould, and to ensure a flat resin front before entering the preform. The constant flow rate experiments were carried out with an Eldo-Mix 101 injection unit from Dopag AG (Cham, CH). The monomer and the hardener were pumped from the containers to the mixing head through heated hoses, thereafter transported through a plastic tube to a pressure transducer and then into the mould from below.

The video acquisition of the injection process was carried out with a Canon PowerShot S70 camera, which acquires 10 frames per second for 30 seconds with a resolution of 640 x 480 pixels. The corresponding resolution in meters was determined for the experiment performed in this work, as $\Omega = 1.31 \cdot 10^{-4}$ m/pixel. The inlet pressure difference was measured every second with a pressure transducer with a sensitivity of 1 kPa, at the inlet of the mould. The sensor was mounted on a heated part in order to keep the desired temperature throughout the process.

IMAGE ANALYSIS

Saturation Analysis

In the present work the Epikote epoxy resin and the glass reinforcement have similar reflective indices around 1.55 and 1.56, respectively. Since air has a different reflective index, voids appear bright compared to the saturated regions, which appear dark like the mould. To determine the saturation profile over the length of the sample at a specific time, the acquired video frame at that time was analysed by an image analysis algorithm programmed in Matlab R2007b [24]. A black and white image was created, where the white pixels represent voids or in general unsaturated regions, whereas black pixels represent regions of full saturation. To measure the degree of saturation for each position z over the length of the reinforcement, saturation was averaged within the width of the sample. The number of white pixels in a column along the sample width was added and the sum divided by the total number of pixels in the column. To represent z in meters instead of pixel, the scale Ω (m/pixel) was used.

Validation

An incomplete filling experiment was conducted to provide a validation sample. The produced laminate was cut into eight bands with cross-sections of 20 x 0.20 mm² at different z -positions separated by 10 mm. Each band was cast in Durofix resin and polished in a Struers Pedemat, Rotopol polishing machine using silicon carbide paper applied in successive steps from 200 to 4000 grit. An Olympus BX-61 optical microscope equipped with a Color View 1 digital camera was used to study and acquire digital images of the cross-sections. The void content was

calculated by the software AnalySIS over the cross-section of each sample, for each z -position studied. The $S(z, t_i)$ data determined from the microscopy analysis could be compared to that calculated from an image of the injected part, taken while still in the mould.

Flow Rate Analysis

To ensure that no leakage and unevenness of the flow propagation disturbed the results, the superficial velocity at the time t_i was directly calculated from the video acquisition after being treated and converted from RGB colours to black and white as described previously. Then, the black and white video frame at time t_i was subtracted from that at time $t_{i+1} = t_i + \Delta t$. The superficial velocity u_s (m s^{-1}) at time t_i was calculated as:

$$u_s = \frac{(1 - V_f) N_{wp} \Omega^2}{h_{\text{frame}} \Delta t}, \quad (6)$$

where N_{wp} is the number of white pixels, h_{frame} (m) the height of the frame.

RESULTS

In all experiments, the measured inlet pressure difference, Δp_{in} showed a linear increase with time, except in the very beginning. This indicates that the flow rate is constant and that Darcy's law can be used to describe the saturated flow, behind the unsaturated region, which is a constant. From the video frames (Fig. 1), the saturation as a function of the position z was calculated by image analysis. The saturation was averaged over each column of pixels, which

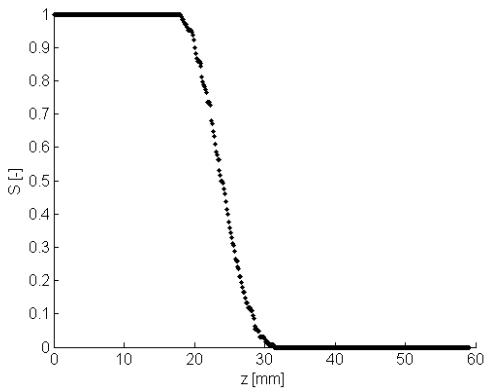


Fig. 2 $S(z)$ calculated by image analysis from the video frame at $t_i = 10$ s.

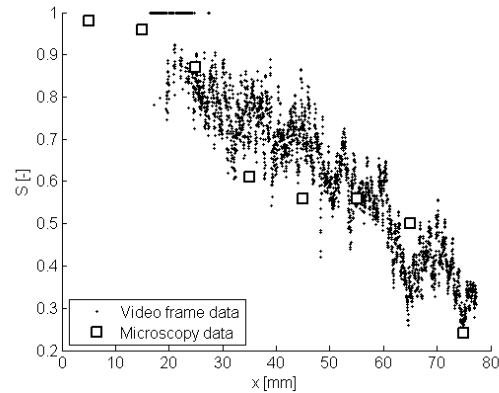


Fig. 3 Measurement of the saturation performed by video frame analysis and microscopic analysis on a cured plate.

lead to a smoothing of the dual-scale fringe behaviour towards a 1D saturation curve in the injection direction, Figure 2. S decreases almost linearly over the unsaturated region. This relates to the almost linear increase in fringe thickness over their lengths as observed in Fig. 1. Fig. 3 presents the comparison of saturation measurement performed by microscopy analysis of the polished cuts and the video analysis method. The large scatter of the video frame data is due to

the use of high resolution images of 3072 x 2304 for the image analysis, and the presence of small pores enclosed inside the fibre bundles of the cured sample. Despite the large scatter, the saturation data determined by the image analysis method shows good agreement with the data acquired by the microscopy analysis. The step like behaviour shown in the microscopy data is a result of the existence of large pores between the fibre bundles. These pores were formed at the end of the injection stage, when air was permitted to enter the sample to create a gradient in the porosity.

Drainage Curve

In order to convert the $S(z, t_i)$ data to $S(p)$ data, numerical simulations of the injection were conducted. The superficial velocity used as inlet boundary condition was calculated from the flow rate calculated from the image analysis, the total cross sectional area seen in the image and the fibre volume fraction. Using the optimal parameter combination calculated by the optimization routine into Equation (3) and (4), the $S(p)$ and the $k_r(S)$ curve are given in Fig. 4a-b respectively, for injection with a superficial velocity of 1.1 mm/s.

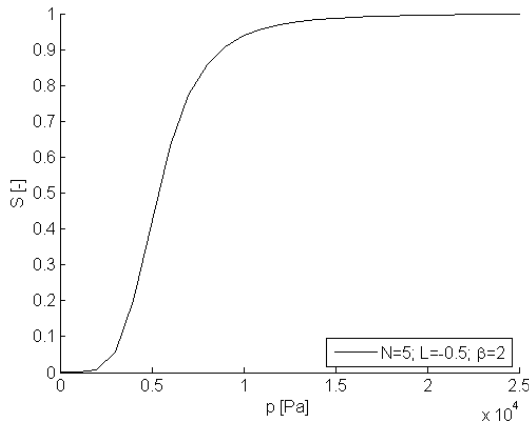


Fig. 4a The optimal $S(p)$ computed by the RSM optimization for the time $t_i = 10$ s.

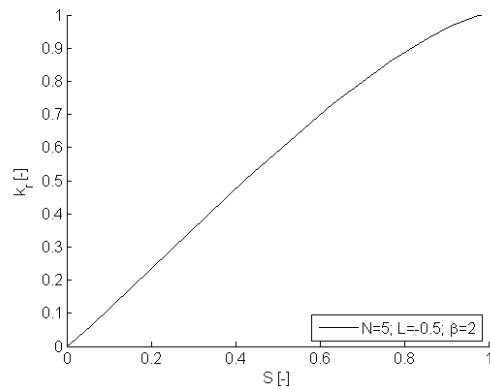


Fig. 4b The optimal $k_r(S)$ computed by the RSM optimization for the time $t_i = 10$ s.

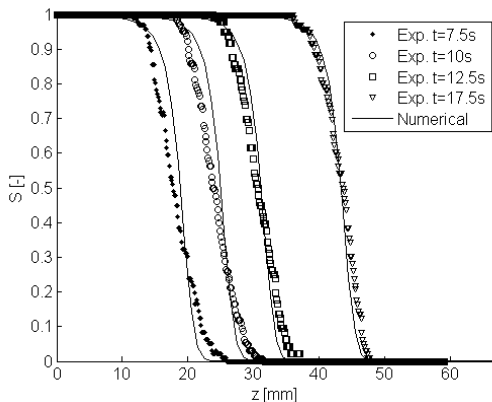


Fig. 5 Experimental and numerical $S(z, t)$.

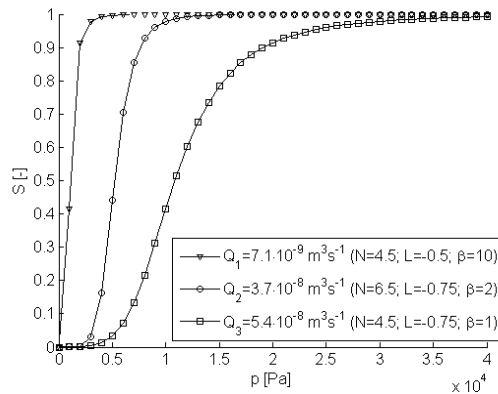


Fig. 6 Saturation curves obtained for three different flow rate conditions.

The relative permeability shows an almost linear dependence on the saturation, as was also found in [15]. In order to verify if the $S(p)$ curve determined after 10 seconds of injection can be used to represent the entire filling, the numerically determined $S(z,t)$ was compared to experimental curves at four times, $t = 7.5$ s, 10 s, 12.5 s and 17.5 s. The numerical curves are all based on the $S(p)$ optimal fit ($N = 5$, $L = -0.5$, $\beta = 2$) calculated at $t = 10$ s, as an input. Fig. 5 shows that the numerical and the experimental data are in good agreement for all times studied. The method can also be used for thicker stacks of fabrics, but with reduced accuracy and over-predicted saturation, due to the two-dimensionality of the image analysis. In this case, optical or X-Ray tomographic systems could be used in a similar way, provided their acquisition time is fast enough. Finally, Fig. 6 presents 3 curves obtained for different cases of superficial velocities, 0.23 mm/s, 1.33 mm/s and 1.7 mm/s. It is observed that the drainage curves are different, with a sharper saturation curve for lower flow rates. This confirms that capillary phenomena in composite processing are velocity dependent.

CONCLUSIONS

A method was presented to determine $S(p)$ and $k_r(S)$ curves by combining video acquisition and pressure measurements of unidirectional, constant flow rate injections of a glass fibre reinforcement by an epoxy resin. The image analysis method to determine $S(z,t_i)$ was validated by microscopy analysis and showed good agreement. The method was demonstrated for one injection condition, where the optimal combination of the parameters of van Genuchten's equations was calculated from the experimental and numerical data. The determined, $S(p)$ and $k_r(S)$ expressions were thereafter used as an input into the simulations. The resulting $S(z,t_i)$ curves compared well with experimental results at other times. This indicates that the method is stable and can be used to determine $S(p)$ and $k_r(S)$ expressions for unsaturated flow of resin into a dual-scale glass fibre fabric.

ACKNOWLEDGEMENTS

Mr. S. Ekdahl is thanked for participation in this work during his Master studies.

REFERENCES

1. Pillai, K.M., "Modeling the Unsaturated Flow in Liquid Composite Molding Processes: A Review and Some Thoughts". *J. of Comp. Materials*. **38**(23): p. 2097-2118, 2004.
2. Binetruy, C., B. Gourichon, and P. Krawczak, "Experimental Investigation of High Fiber Tow Count Fabric Unsaturation during RTM". *Composites Science and Technology*, **66**(7-8): p. 976-82, 2006.
3. Parnas, R.S., et al., "Permeability Characterization. Part 1: A Proposed Standard Reference Fabric for Permeability". *Polymer Composites*. **16**(6): p. 429-445, 1995.
4. Kuentzer, N., et al., "Permeability Characterization of Dual Scale Fibrous Porous Media". *Composites Part A*, **37**(11): p. 2057-2068, 2006.
5. Zhou, F.P., et al., "Analytic Characterization of the Permeability of Dual-Scale Fibrous Porous Media". *Composites Science And Technology*, **66**(15): p. 2795-2803, 2006.

6. Bear, J. and Y. Bachmat, "Introduction to Modeling of Transport Phenomena in Porous Media". Dordrecht: Kluwer Academic Publishers, 1991.
7. Greenkorn, R.A., "Flow Phenomena in Porous Media". N.Y. Marcel Dekker, 1983.
8. Michaud, V. and A. Mortensen. "Infiltration Processing of Fibre Reinforced Composites: Governing Phenomena". *Composites part A*, 32 , pp.981-996, 2001.
9. Li, K., "Generalized Capillary Pressure and Relative Permeability Model Inferred from Fractal Characterization of Porous Media". SPE paper No. 89874, 2004.
10. Bear, J., "Dynamics of Fluids in Porous Media", New York: American Elsevier, 1972.
11. Scheidegger, A.E., "The Physics of Flow through Porous Media". University of Toronto Press, 1974.
12. Dullien, F.A.L., "Porous Media, Fluid Transport and Pore Structure". New York: Academic Press, 1979.
13. Bahraini, M., et al., "Measuring and Tailoring Capillary Forces during Liquid Metal Infiltration". *Current Opinion in Solid State and Mat. Sci.* **9**(4-5): p. 196, 2005.
14. Bahraini, M., et al., "Wetting in Infiltration of Alumina Particle Preforms with Molten Copper". *Journal of Materials Science*, 2005. **40**(9 - 10): p. 2487.
15. Dopler, T., A. Modaressi, and V. Michaud, "Simulation of Metal-Matrix Composite Isothermal Infiltration Processing". *Metallurgical and Materials Transactions B*, 2000. **31**(2): p. 225-234.
16. Michaud, V.J., L.M. Compton, and A. Mortensen, "Capillarity in Isothermal Infiltration of Alumina Fiber Preforms with Aluminum". *Met. and Mat. Transactions A: Physical Metallurgy and Materials Science*, **25A**(10): p. 2145-2152, 1994.
17. Patel, N. and L.J. Lee, "Modeling of Void Formation and Removal in Liquid Composite Molding. Part II: Model Development and Implementation". *Polymer Composites*, **17**(1): p. 104-114, 1996.
18. Brooks, R.H. and A.T. Corey, "Hydraulic Properties of Porous Media". *American Society of Agricultural Engineers -- Transactions*, 1964. **7**(1): p. 26-28.
19. van Genuchten, M.T., "Closed Form Equation for Predicting the Hydraulic Conductivity of Unsaturated Soils". *Soil Science Society of America J.*, **44**(5): p. 892-898, 1980.
20. Michaud, V. and A. Mortensen, "On measuring wettability in infiltration processing." *Scripta Materialia*. **56**(10): p. 859-62, 2007.

21. Patel, N. and L.J. Lee, "Modeling of Void Formation and Removal in Liquid Composite Molding. Part I: Wettability Analysis". *Polymer Composites*, **17**(1): p. 96-103, 1996.
22. Labat, L., et al., "Void Fraction Prevision in LCM Parts". *European Physical Journal-Applied Physics*, **16**(2): p. 157-164, 2001.
23. Labat, L., et al., "Original Use of Electrical Conductivity for Void Detection Due to Injection Conditions of Composite Materials". *Comptes Rendus De L Academie Des Sciences Serie II Fascicule B-Mecanique*, **329**(7): p. 529-534, 2001.
24. Nordlund, M., V. Michaud and J.-A.E. Månson, "Dynamic Saturation Curve Measurement During Resin Flow in Glass Reinforcement", *subm. to Comp. Part A.*, 2008.
25. Mualem, Y., "Hydraulic Conductivity of Unsaturated Porous Media: Generalized Macroscopic Approach". *Water Resources Research*, **14**(2): p. 325-34, 1978.
26. Verrey, J., V. Michaud, and J.A.E. Manson, "Dynamic Capillary Effects in Liquid Composite Moulding with Non-Crimp Fabrics", *Comp. Part A*, **37**(1): p. 92-102, 2006.